

# **Stabilizing the Garnet Solid-Electrolyte / Polysulfide Interface in Li-S Batteries**

Kun (Kelvin) Fu,<sup>1,2,(a)</sup> Yunhui Gong,<sup>1,2,(a)</sup> Shaomao Xu,<sup>1,2,(a)</sup> Yizhou Zhu,<sup>2</sup> Yiju Li,<sup>2</sup> Jiaqi Dai,<sup>2</sup> Chengwei Wang,<sup>1,2</sup> Boyang Liu,<sup>2</sup> Glenn Pastel,<sup>2</sup> Hua Xie,<sup>2</sup> Yonggang Yao,<sup>2</sup> Yifei Mo,<sup>1,2</sup> Eric Wachsman,<sup>1,2,\*</sup> Liangbing Hu<sup>1,2,\*</sup>

<sup>1</sup>University of Maryland Energy Research Center, University of Maryland, College Park, Maryland, 20742

<sup>2</sup>Department of Materials Science and Engineering, University of Maryland, College Park, Maryland, 20742

<sup>(a)</sup> Equally contributed

\* Corresponding author: [binghu@umd.edu](mailto:binghu@umd.edu); [ewach@umd.edu](mailto:ewach@umd.edu)

## Experimental

**Garnet solid-state electrolyte preparation.** The LLCZN powder was synthesized *via* a modified sol-gel method. The starting materials were  $\text{LiNO}_3$  (99%, Alfa Aesar),  $\text{La}(\text{NO}_3)_3$  (99.9%, Alfa Aesar),  $\text{Ca}(\text{NO}_3)_2$  (99.9%, Sigma Aldrich),  $\text{ZrO}(\text{NO}_3)_2$  (99.9%, Alfa Aesar) and  $\text{NbCl}_5$  (99.99%, Alfa Aesar). Stoichiometric amounts of these chemicals were dissolved in de-ionized water and 10% excess  $\text{LiNO}_3$  was added to compensate for lithium volatilization during the high temperature pellet preparation. Citric acid and ethylene glycol (1:1 mole ratio) were added to the solution. The solution was evaporated at  $120^\circ\text{C}$  for 12h to produce the precursor gel and then calcined to  $400^\circ\text{C}$  and  $800^\circ\text{C}$  for 5 hours to synthesize the garnet powder. The garnet powders were uniaxially pressed into pellets and sintered at  $1050^\circ\text{C}$  for 12 hours covered by the same type of powder for conductivity and stability experiments.

**Material characterization.** Phase analysis was performed by powder X-ray diffraction (XRD) on a D8 Advanced with LynxEye and SolX (Bruker AXS, WI, USA) using a  $\text{Cu K}\alpha$  radiation source operated at 40 kV and 40 mA. The morphology of the samples was examined by a field emission scanning electron microscope (FE-SEM, JEOL 2100F). Raman characterization was done with a Horiba Jobin-Yvon with the laser wavelength at 532 nm and the integration time of 4 seconds repeated for 4 times.

**First Principles Computation.** We considered the interface as a pseudo-binary of  $\text{Li}_2\text{S}/\text{Li}_2\text{S}_8$  and garnet using the same approach as defined in previous work.<sup>26</sup> The phase diagrams were constructed to identify possible thermodynamically favorable reactions. The energies for the materials used in our study were obtained from the Materials Project (MP) database<sup>30</sup>, and the compositional phase diagrams were constructed using the *pymatgen* package<sup>31</sup>. The mutual

reaction energy of the pseudo-binary was calculated using the same approach as defined in our previous work<sup>26</sup>.

**Electrochemical characterization.** To measure the ionic conductivity of the garnet solid-state electrolyte, an Au paste was coated on both sides of the dense ceramic disk and acted as a blocking electrode. The gold electrodes were sintered at 700°C to form good contact with the ceramic pellet. Conductivities were calculated using  $\sigma = L/(Z \times A)$ , where  $Z$  is the impedance for the real axis in the Nyquist plot,  $L$  is the garnet ceramic disk length, and  $A$  is the surface area. The activation energies were obtained from the conductivities as a function of temperature using the Arrhenius equation. The hybrid solid-state cells were prepared in argon-filled glove box. 1M bis(trifluoromethane)sulfonimide lithium salt (LiTFSI, Sigma) in a mixture of dimethoxyethane (DME) and 1,3-dioxolane (DOL) (1:1 by volume) was used as the electrolyte for the hybrid solid-state Li-S batteries. Galvanostatic discharging and charging was measured using a cut-off voltage window of 1-3.5 V. The cell was then assembled into a 2032 coin cell with a highly conductive carbon sponge. The carbon sponge acted as the force absorber and prevented the garnet ceramic disk from being damaged. Battery test clips were used to hold and provide good contact with the coin cell. The edge of the cell was sealed with epoxy resin.

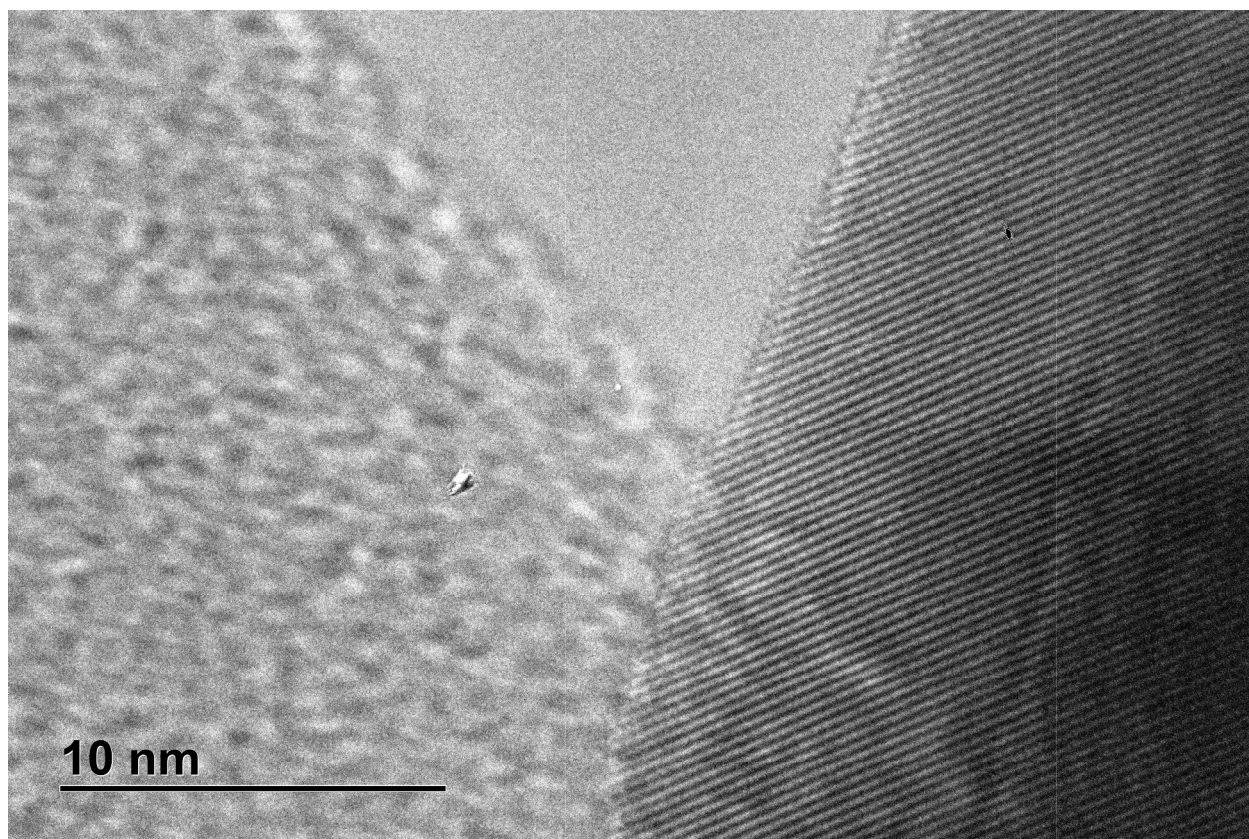


Figure S1. TEM of pristine garnet, showing highly crystallized grain and no amorphous region on surface.

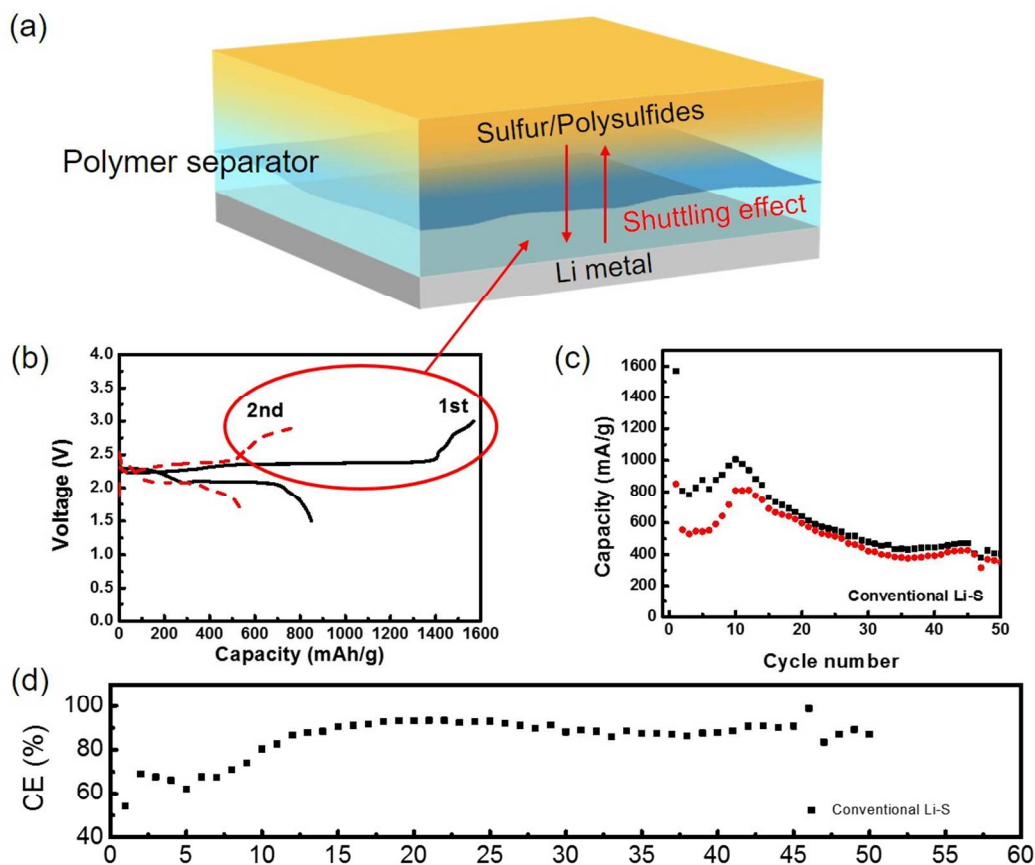


Figure S2. Control experiment of conventional Li-S battery using polymer separator membrane. The sulfur mass loading is  $\sim 1.2 \text{ mg/cm}^2$ . (a) Schematic of shuttling effect in conventional Li-S battery. (b) Voltage profiles of conventional Li-S battery with a long charge plateau, indicating the shuttling effect of polysulfides. (c) Cycling performance of the conventional Li-S cell. The cell shows a fast decay after 10 cycles. (d) Coulombic efficiency of the conventional Li-S cell.

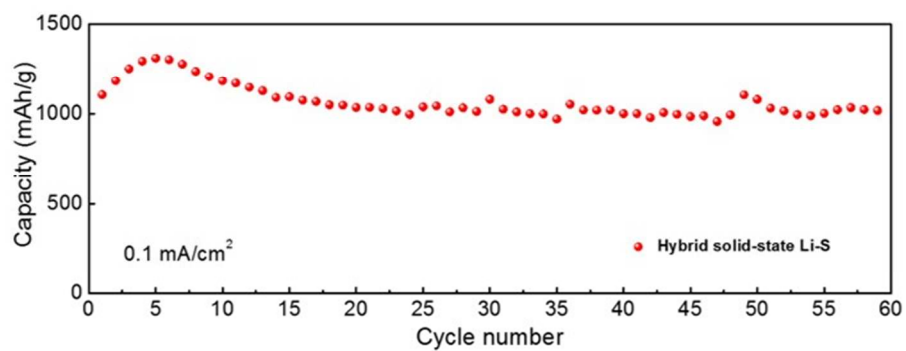


Figure S3. Cycling performance of hybrid garnet solid-state Li-S battery at a current of 0.1 mA/cm<sup>2</sup>. The sulfur loading is 1.2 mg/cm<sup>2</sup>. The hybrid cell delivered high capacity >1000 mAh/g with negligible capacity fade over 60 cycles, demonstrating no polysulfide shuttling.

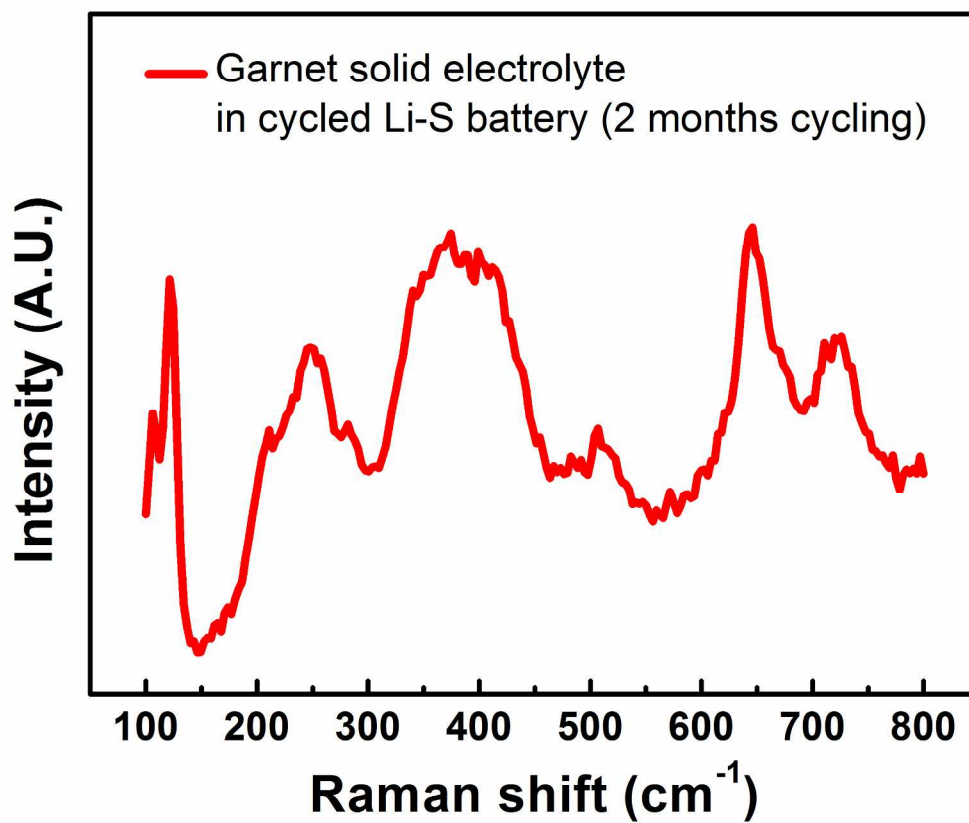


Figure S4. Raman spectrum of cycled garnet solid electrolyte in Li-S battery over 2 months cycling.

**Table S1.** The phase equilibria and decomposition energies of the Li-garnet  $\text{Li}_7\text{La}_3\text{Zr}_2\text{O}_{12}$  and polysulfide  $\text{Li}_2\text{S}_8$ . Ratio  $x$  is the molar fraction of Li-garnet  $\text{Li}_7\text{La}_3\text{Zr}_2\text{O}_{12}$  in the pseudo-binary composition (The parent composition of  $\text{Li}_7\text{La}_3\text{Zr}_2\text{O}_{12}$  and polysulfide  $\text{Li}_2\text{S}_8$  are already normalized to one atom per formula).

Ratio $x$	$\Delta E_{\text{D,mutual}}$ (meV/atom)	Phase Equilibria
0.520	-262.582	$\text{Li}_2\text{S}$ , $\text{LaS}_2$ , $\text{ZrS}_3$ , $\text{Li}_2\text{SO}_4$
0.639	-246.345	$\text{Li}_2\text{S}$ , $\text{ZrO}_2$ , $\text{LaS}_2$ , $\text{Li}_2\text{SO}_4$
0.721	-219.383	$\text{Li}_2\text{S}$ , $\text{ZrO}_2$ , $\text{LaSO}$ , $\text{Li}_2\text{SO}_4$
0.771	-201.855	$\text{Li}_2\text{S}$ , $\text{ZrO}_2$ , $\text{La}_2\text{SO}_2$ , $\text{Li}_2\text{SO}_4$
0.808	-181.707	$\text{Li}_2\text{S}$ , $\text{Li}_2\text{SO}_4$ , $\text{La}_2\text{SO}_2$ , $\text{La}_2\text{Zr}_2\text{O}_7$
0.848	-156.986	$\text{Li}_2\text{S}$ , $\text{La}_2\text{SO}_2$ , $\text{Li}_2\text{ZrO}_3$ , $\text{Li}_2\text{SO}_4$
0.894	-119.624	$\text{Li}_6\text{Zr}_2\text{O}_7$ , $\text{Li}_2\text{SO}_4$ , $\text{La}_2\text{SO}_2$ , $\text{Li}_2\text{S}$
0.909	-103.100	$\text{Li}_6\text{Zr}_2\text{O}_7$ , $\text{Li}_2\text{SO}_4$ , $\text{La}_2\text{SO}_2$ , $\text{Li}_2\text{O}$

ToC

